Nonlinear Dyn (2016) 83:217–230
DOI 10.1007/s11071-015-2321-9

ORIGINAL PAPER

A modified dynamical formulation for two-wheeled self-balancing robots

Ali Ghaffari · Azadeh Shariati · Amir H. Shamekhi

Received: 24 December 2014 / Accepted: 6 August 2015 / Published online: 20 August 2015

Abstract Two-wheeled self-balancing robot, moving on a horizontal plane, may be presented by a set of highly coupled nonlinear differential equations. In the recent literatures and in the commonly used two-wheeled self-balancing robots, the control algorithms are designed based on the mathematical models with simplified structure. In these models, a nonlinear coupling term is usually neglected, whereas it has significant effects on the dynamic behavior of the system. In this paper, the mathematical representation of two-wheeled self-balancing robots, including this new term, is derived using both Kane's and Lagrangian methods. The significant effect of the new term on the response of the system is shown by presenting the behavior of the system under different conditions and by comparing it with the system models when this term is neglected. Then sliding-mode control techniques are used to derive the controllers. The controller objective is to drive the two-wheeled self-balancing robot to the desired path as well as to make the robot stable. By some simulations, the behavior of the robot with the proposed controller is discussed. It is shown that if the nonlinear coupling term is ignored in designing the controller, the controller cannot compensate its effect.

A. Ghaffari · A. Shariati (✉) · A. H. Shamekhi
Department of Mechanical Engineering, Center of Excellence in Robotics and Control, K. N. Toosi University of Technology, Tehran 19697, Iran
e-mail: azadeh_sht@yahoo.com; azadeh.shariati@mail.kntu.ac.ir

Keywords Dynamical equations · Kane's method · Lagrangian method · Two-wheeled self-balancing robot · Sliding-mode controller

1 Introduction

Due to the nonholonomic constraints and inherent instability, the problem of two-wheeled robot is an interesting and challenging case in control and dynamic systems. Some practical two-wheeled self-balancing robots are the JOE [1], the B2 [2], and the commercial product Segway [3], etc. Generally the equations of motion of wheeled robots with unstable chassis (inverted pendulum) are coupled and convoluted. This complexity arises from two factors: nonholonomic constraints and complicated mechanism. Many researchers have been devoted to the stability analysis and control system design of the two-wheeled self-balancing robots. However, fewer investigations have been devoted to the problem of dynamical modeling. In the field of control, Ravichandran and Mahindrakar presented a controller design and employed a strategy that combines time scaling and Lyapunov redesign. They verified the methodology by employing it in a two-wheeled robot [4]. Maddahi et al. [5] investigated the design and validation of a controller for an inertial two-wheeled vehicle using the Lyapunov's feedback control design technique. The existence, continuity, and uniqueness of the solution for the proposed control system are proved utilizing the Filippov's solution.

Huang et al. [6] improved a robust-velocity-tracking by proposing two sliding-mode control methods. Cui et al. [7] designed a backstepping-based adaptive control to achieve tracking for the two-wheeled self-balancing robot. Yue et al. considered the overall dynamical model of Grasser [1], as three subsystems: rotational motion, longitudinal motion, and zero dynamics. Particularly, the inclination angle of the chassis is treated as zero dynamics where the longitudinal acceleration is taken as the control input. Then the sliding-mode control techniques are used to derive the controllers [8]. In another paper they employed adaptive laws for the design parameters beside the sliding-mode controllers [9].

In the field of dynamical modeling, many researchers are devoted to the modeling of the two-wheeled mechanisms, which has more degrees of freedom compared with the regular two-wheeled self-balancing robot. A regular two-wheeled self-balancing robot has two actuated drive wheels connected to an intermediate chassis. Goher et al. [10] employed Lagrangian approach for dynamical modeling of two-wheeled robots and added more degrees of freedom in comparison with the works done by the former researchers. Larimi et al. [11] presented a new stabilization mechanism of two-wheeled mobile robots, where a reaction wheel is considered to control the position of center of gravity (*CoG*). Almeshal et al. [12] employed Lagrangian approach for dynamical modeling of two-wheeled robots and added more degrees of freedom in comparison with the works done by the former researchers. Huang et al. [13] investigated a novel narrow vehicle based on a two-wheeled robot and a movable seat. The dynamic model of the vehicle is derived by Lagrange's equation of motion.

On the dynamical modeling of the regular two-wheeled self-balancing robot, Grasser [1] derived a dynamic model of the system using Newtonian approach and linearized the equations around an operating point to design a controller. Pathak [14] analyzed the dynamic model from a controllability and feedback linearizability point of view. Kim et al. [15] investigated the dynamics of the robot with the aid of Kane's method. Kim's formulation is used by many researchers for their control purposes.

In this paper, we derive a modified formulation for two-wheeled self-balancing robots and compare our results with Kim's formulation. We will show that there is a term which is not considered in the reference [15] and in the other related references. The existence of this term is proved by obtaining dynamical equations with both Lagrangian approach and Kane's method. The importance of the new term is examined by presenting its effects on the free response of the system and by applying sliding-mode controllers.

The content of this article is organized as follows: In Sect. 2, the system is described and dynamical equations are derived, using both Kane's method and Lagrangian approach, and open-loop simulation results are presented; Sect. 3 is devoted to the design of sliding-mode controllers, and finally, conclusions are presented in Sect. 4.

2 System description and dynamical representation

Two-wheeled robot which is analyzed in this article is a chassis mounted on the top of an axel incorporating two wheels where the chassis has no balancing support. The robot is powered by two DC motors driving the robot wheels. It has four degrees of freedom, three degrees are due to the movement of the wheels on the horizontal plane (including two positions and the steering angle of the chassis), and the fourth degree is due to the inclination angle of the unstable chassis which acts like an inverted pendulum (DOF = 4) (see Figs. 1, 2). However, the system has three differentiable degrees of freedom (DDOF = 3), which means that the system has three independent achievable velocities [16]. The independent velocity of a two-wheeled self-balancing robot can be represented with three axes, one representing the instantaneous longitudinal velocity, the second

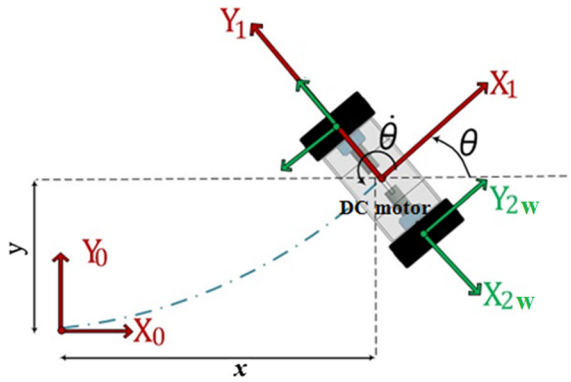

Fig. 1 Robot and road reference frame

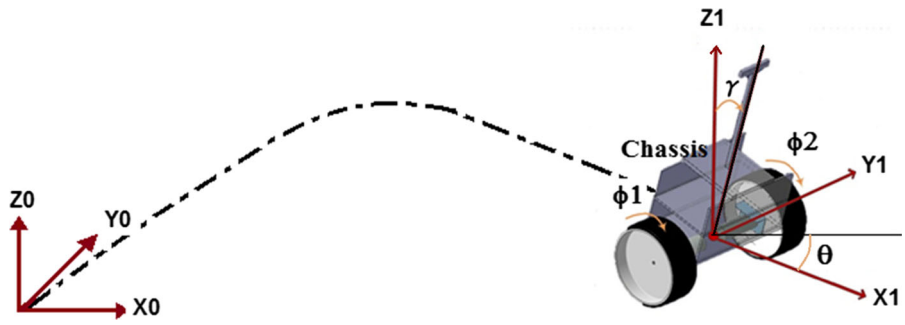

Fig. 2 Representation of the robot and configuration parameters

representing the instantaneous steering angular velocity of the robot, and the third representing the instantaneous change of the inclination angle of the chassis. We define the configuration variables of the system initially as $[x, y, \theta, \gamma, \varphi_1, \varphi_2]^{\mathrm{T}}$, where x and y are the position of the system in the horizontal plane (midway between the two wheels' center), θ is the steering angle of the chassis, measured from the inertial x-axis, and γ is the attitude, or the inclination angle of the chassis measured from the z-axis. Parameters φ_1 and φ_2 are the rotational angles of the first wheel and the second one, respectively (see Figs. 1, 2). The chassis parameters have the subscript 'ch,' and the wheel parameters have the subscript 'w.' The motion of the two-wheeled robot is described by a set of second-order differential equations, and the nonlinear dynamics of the chassis is coupled with the dynamics of the wheels. The following assumptions have been considered in modeling this system:

- The body of the system is assumed to be symmetric with respect to the X_1Z_1 plane and Y_1Z_1 plane (see Fig. 1).
- Slip in tires is ignored.
- Chassis can rotate freely around wheel axes, i.e., the impact with the ground is ignored. In practice, if there are no actuating forces on the system, then angle γ cannot be $>90°$; because the arm has contact with the ground, but by considering $h + h' < r_{\mathrm{w}}$, this contact will not happen, where h is distance from central point of the line between the two wheels to CoG of the chassis, h' is distance from CoG of the chassis to the top of the chassis, i.e., $h + h'$ is distance from central point of the line between the two wheels to the top of the chassis, and r_{w} is radius of the wheels (see Fig. 3).

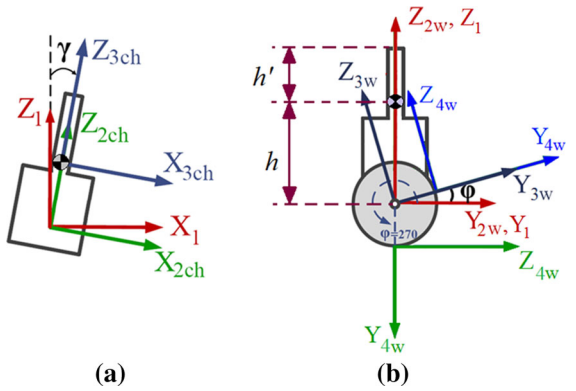

Fig. 3 Representation of coordinate systems. **a** Chassis' frames. **b** Wheel's frames

2.1 Kinematics

2.1.1 Chassis kinematics

For kinematic analysis of the robot, we use those coordinate systems which are shown in Figs. 1 and 2. The frame $X_0Y_0Z_0$ is the inertial reference frame. The frame $X_1Y_1Z_1$ is attached to the chassis, midway between the two wheels' center, and rotates θ degree around Z_0 axis. Distance from the origin of the frame $X_0Y_0Z_0$ to the origin of the frame $X_1Y_1Z_1$ is equal to $[x, y, r_{\mathrm{w}}]$. For kinematic analysis of the chassis, we need to define coordinate systems $X_{2_{\mathrm{ch}}}Y_{2_{\mathrm{ch}}}Z_{2_{\mathrm{ch}}}$ and $X_{3_{\mathrm{ch}}}Y_{3_{\mathrm{ch}}}Z_{3_{\mathrm{ch}}}$. Frame $X_{2_{\mathrm{ch}}}Y_{2_{\mathrm{ch}}}Z_{2_{\mathrm{ch}}}$ is attached to the chassis as well as its center is attached to the center of the frame $X_1Y_1Z_1$. The pitch angle of γ is $\angle\left(Z_1, Z_{2_{\mathrm{ch}}}\right)$. Frame $X_{3_{\mathrm{ch}}}Y_{3_{\mathrm{ch}}}Z_{3_{\mathrm{ch}}}$ has the same direction as $X_{2_{\mathrm{ch}}}Y_{2_{\mathrm{ch}}}Z_{2_{\mathrm{ch}}}$, and its origin locates on the center of mass of the chassis. The distance between the origin of $X_{2_{\mathrm{ch}}}Y_{2_{\mathrm{ch}}}Z_{2_{\mathrm{ch}}}$ and the origin of $X_{3_{\mathrm{ch}}}Y_{3_{\mathrm{ch}}}Z_{3_{\mathrm{ch}}}$ is equal to h.

Referring to the defined coordinates, transform matrixes are given as (47)–(49) (see Appendix 1).

The relative linear and angular velocities are obtained as (50) and (51). The angular velocity of the chassis and the linear velocity of the center of mass of the chassis are presented by (1) and (2), correspondingly:

$$ {}^{3_{\mathrm{ch}}}v_{\mathrm{ch}} = \begin{bmatrix} \cos\gamma(\dot{x}\ \cos\theta + \dot{y}\ \sin\theta) + \dot{\gamma}h \\ -\dot{x}\ \sin\theta + \dot{y}\ \cos\theta + \dot{\theta}\,h\ \sin\gamma \\ \sin\gamma\ (\dot{x}\ \cos\theta + \dot{y}\ \sin\theta) \end{bmatrix} \tag{1} $$

$$ {}^{3_{\mathrm{ch}}}w_{\mathrm{ch}} = \begin{bmatrix} -\dot{\theta}\sin\gamma \\ \dot{\gamma} \\ \dot{\theta}\cos\gamma \end{bmatrix} \tag{2} $$

2.1.2 Wheel kinematics

For kinematic analyzing of the wheels, we define the coordinate systems $X_{2_{\mathrm{w}}}Y_{2_{\mathrm{w}}}Z_{2_{\mathrm{w}}}$, $X_{3_{\mathrm{w}}}Y_{3_{\mathrm{w}}}Z_{3_{\mathrm{w}}}$, and $X_{4_{\mathrm{w}}}Y_{4_{\mathrm{w}}}Z_{4_{\mathrm{w}}}$ (see Fig. 3). The frame $X_{2_{\mathrm{w}}}Y_{2_{\mathrm{w}}}Z_{2_{\mathrm{w}}}$ is accessed by a rotation equal to α about Z_1 axis and a transition equal to l along Y_1 axis, where l is half-distance between wheels. The frame $X_{3_{\mathrm{w}}}Y_{3_{\mathrm{w}}}Z_{3_{\mathrm{w}}}$ is attached to the center of gravity of the wheels and rotates with wheels, with the angular velocity equal to $\dot{\varphi}$. Referring to the defined frames, we obtain the transform matrixes as (52)–(54) and the relative linear and angular velocities as (55) and (56) (see Appendix 1).

The linear velocity of the center of mass of the wheels and the angular velocities, in their body frames, are obtained as (3) and (4), respectively. For the first wheel, $\alpha = \frac{\pi}{2}$ and $\varphi = -\varphi_1$, and for the second wheel, $\alpha = \frac{3\pi}{2}$ and $\varphi = \varphi_2$.

$$ {}^{3_{\mathrm{w}}}v_{\mathrm{w}} = \begin{bmatrix} \dot{x}\cos(\theta+\alpha) + \dot{y}\ \sin(\theta+\alpha) \\ \cos\ \varphi[-\dot{x}\ \sin\ (\theta+\alpha)+\dot{y}\cos(\theta+\alpha)+l\,\dot{\theta}] \\ -\sin\ \varphi\left[-\dot{x}\ \sin\ (\theta+\alpha)+\dot{y}\cos(\theta+\alpha)+l\,\dot{\theta}\right] \end{bmatrix} \tag{3} $$

$$ {}^{3_{\mathrm{w}}}\omega_{\mathrm{w}} = \begin{bmatrix} \dot{\varphi} \\ \dot{\theta}\sin\ \varphi \\ \dot{\theta}\cos\ \varphi \end{bmatrix} \tag{4} $$

2.1.3 Constraint equations

Coordinate system $X_{4_{\mathrm{w}}}Y_{4_{\mathrm{w}}}Z_{4_{\mathrm{w}}}$ is used for governing constraint equations. It is obtained by transition of the origin of the frame $X_{3_{\mathrm{w}}}Y_{3_{\mathrm{w}}}Z_{3_{\mathrm{w}}}$ equal to $-r_{\mathrm{w}}$ along $Y_{3_{\mathrm{w}}}$ axis and substituting $\varphi = 270$. Then the center of frame $X_{4_{\mathrm{w}}}Y_{4_{\mathrm{w}}}Z_{4_{\mathrm{w}}}$ settles on the ground. The velocity of the origin of the frame $X_{4_{\mathrm{w}}}Y_{4_{\mathrm{w}}}Z_{4_{\mathrm{w}}}$ is given by;

$$ {}^{4_{\mathrm{w}}}v_{4_{\mathrm{w}}} = \begin{bmatrix} \dot{x}\cos(\theta+\alpha)+\dot{y}\ \sin(\theta+\alpha)-r_{\mathrm{w}}\dot{\theta}\cos\ \varphi \\ -\dot{x}\ \sin\ (\theta+\alpha)\cos\ \varphi+\dot{y}\cos(\theta+\alpha)\cos\ \varphi+l\,\dot{\theta}\cos\ \varphi \\ \dot{x}\ \sin\ (\theta+\alpha)\sin\varphi-\dot{y}\ \cos(\theta+\alpha)\ \sin\varphi-l\,\dot{\theta}\sin\ \varphi+r_{\mathrm{w}}\dot{\varphi} \end{bmatrix} \tag{5} $$

For the first wheel, we have $\varphi = \frac{3k\pi}{2}$, $\alpha = \frac{\pi}{2}$, so,

$$ {}^{4_{\mathrm{w}}}v_{4_{\mathrm{w}}\ |1\mathrm{st\ wheel}} = \begin{bmatrix} -\dot{x}\ \sin\ \theta+\dot{y}\ \cos\theta \\ 0 \\ -\dot{x}\ \cos\ \theta-\dot{y}\ \sin\theta+l\,\dot{\theta}+r_{\mathrm{w}}\dot{\varphi}_1 \end{bmatrix} = \begin{bmatrix} 0 \\ 0 \\ 0 \end{bmatrix} \tag{6} $$

For the second wheel, we have $\varphi = \frac{3k\pi}{2}$, $\alpha = \frac{3\pi}{2}$, so

$$ {}^{4_{\mathrm{w}}}v_{4_{\mathrm{w}}\ |2\mathrm{nd\ wheel}} = \begin{bmatrix} \dot{x}\ \sin\ \theta-\dot{y}\ \cos\theta \\ 0 \\ \dot{x}\ \cos\ \theta+\dot{y}\ \sin\theta+l\,\dot{\theta}+r_{\mathrm{w}}\dot{\varphi}_2 \end{bmatrix} = \begin{bmatrix} 0 \\ 0 \\ 0 \end{bmatrix} \tag{7} $$

Considering the no-slip condition, at the point of contact, the velocity of the wheels is equal to zero in all directions. Thus, the constraint equations can be written as:

$$ -\dot{x}\ \sin\ \theta+\dot{y}\ \cos\theta = 0 \tag{8a} $$

$$ \dot{x}\ \cos\ \theta+\dot{y}\ \sin\theta-l\,\dot{\theta} = r_{\mathrm{w}}\dot{\varphi}_1 \tag{8b} $$

$$ \dot{x}\ \cos\ \theta+\dot{y}\ \sin\theta+l\,\dot{\theta} = r_{\mathrm{w}}\dot{\varphi}_2 \tag{8c} $$

2.2 Lagrangian approach

The Lagrange equation can be written as:

$$ \frac{\mathrm{d}}{\mathrm{d}t}\left(\frac{\partial L}{\partial\dot{q}_i}\right) - \frac{\partial L}{\partial q_i} = Q_i + \sum_{j=1}^{N-N_0}\lambda_j\,f_{ij}\ \ (i=1,\ldots,N) \tag{9} $$

where $L = T - U$ is the Lagrangian. Parameters T, U, Q_i, λ_i, f_{ij}, N, N_0, and q_i denote, respectively, the kinetic energy, the gravitational potential energy, the generalized force, the Lagrange multipliers, constraint equation multiplayer, number of coordinates required, degree of freedom, and generalized coordinates; and parameter $s = N - N_0$ is number of con-

Table 1 Lagrange multipliers

f_{ij}	$j=1$	$j=2$	$j=3$
$i=1$	$-\sin\theta$	$-\cos\theta$	$-\cos\theta$
$i=2$	$+\cos\theta$	$-\sin\theta$	$-\sin\theta$
$i=3$	0	l	$-l$
$i=4$	0	r_{w}	0
$i=5$	0	0	r_{w}
$i=6$	0	0	0

straints. A nonholonomic constraint can be expressed as:

$$\sum_{j=1}^{N} f_{ij}\delta q_j = 0 \quad i = 1, \ldots, N - N_0 \tag{10}$$

By comparing (8) and (10), the Lagrange multipliers will be obtained as given in Table 1.

In the Lagrange's method, the scalar energy quantity of a system should be clarified [17]. By computing linear and angular velocity vectors of all rigid bodies, the total kinetic energy of the system is obtained as:

$$\begin{aligned} T_{\mathrm{total}} = {} & \frac{(2m_{\mathrm{w}} + m_{\mathrm{ch}})}{2}\left(\dot{x}^2 + \dot{y}^2\right) \\ & + \frac{I_{1_{\mathrm{w}}}}{2}\left(\dot{\varphi}_1^2 + \dot{\varphi}_2^2\right) + \left(I_{2_{\mathrm{w}}} + m_{\mathrm{w}} l^2\right)\dot{\theta}^2 \\ & + \frac{1}{2}\left(I_{xx_{\mathrm{ch}}} + m_{\mathrm{ch}} h^2\right)\dot{\theta}^2 \sin^2\gamma \\ & + \frac{1}{2}\left(I_{yy_{\mathrm{ch}}} + h^2 m_{\mathrm{ch}}\right)\dot{\gamma}^2 + \frac{1}{2} I_{zz_{\mathrm{ch}}}\dot{\theta}^2\cos^2\gamma \\ & + m_{\mathrm{ch}} h\dot{\gamma}\cos\gamma\,(\dot{x}\,\cos\theta + \dot{y}\,\sin\theta) \\ & + m_{\mathrm{ch}} h\dot{\theta}\sin\gamma\,(-\dot{x}\,\sin\theta + \dot{y}\,\cos\theta) \end{aligned} \tag{11}$$

where $I_{xx_{\mathrm{ch}}}$, $I_{yy_{\mathrm{ch}}}$, and $I_{zz_{\mathrm{ch}}}$, denote, respectively, inertia moment of the chassis relative to axes $X_{3_{\mathrm{ch}}}$, $Y_{3_{\mathrm{ch}}}$, and $Z_{3_{\mathrm{ch}}}$; $I_{1_{\mathrm{w}}}$ and $I_{2_{\mathrm{w}}}$ denote inertia moment of the wheel relative to axes $X_{4_{\mathrm{w}}}$ and $Y_{4_{\mathrm{w}}}$; and m_{ch} and m_{w} denote mass of the chassis and mass of the wheel. The gravitational potential energy of the system is:

$$U_{\mathrm{total}} = m_{\mathrm{ch}} g\, h\, \cos\gamma + m_{\mathrm{ch}}\, g\, h \tag{12}$$

where g is acceleration of gravity. Employing (9), we derive six equations as:

$$\begin{aligned} & (2m_{\mathrm{w}} + m_{\mathrm{ch}})\ddot{x} + m_{\mathrm{ch}} h\,(\ddot{\gamma}\cos\gamma\,\cos\theta \\ & \quad - \dot{\gamma}^2\sin\gamma\cos\theta - \ddot{\theta}\sin\gamma\sin\theta \\ & \quad - 2\dot{\gamma}\dot{\theta}\cos\gamma\,\sin\theta - \dot{\theta}^2\sin\gamma\cos\theta\Big) \\ & = -\sin\theta\,\lambda_1 - \cos\theta\,\lambda_2 - \cos\theta\,\lambda_3 \end{aligned} \tag{13a}$$

$$\begin{aligned} & (2m_{\mathrm{w}} + m_{\mathrm{ch}})\ddot{y} + h m_{\mathrm{ch}}\Big[\left(-\dot{\theta}^2 - \dot{\gamma}^2\right)\sin\gamma\sin\theta \\ & \quad + 2\dot{\theta}\dot{\gamma}\cos\gamma\cos\theta + \ddot{\gamma}\cos\gamma\sin\theta + \ddot{\theta}\sin\gamma\cos\theta\Big] \\ & = \cos\theta\,\lambda_1 - \sin\theta\lambda_2 - \sin\theta\lambda_3 \end{aligned} \tag{13b}$$

$$\begin{aligned} & 2(m_{\mathrm{w}} l^2 + I_{2_{\mathrm{w}}})\ddot{\theta} + \left(I_{xx_{\mathrm{ch}}} + m_{\mathrm{ch}} h^2\right)\,\sin^2\gamma\ddot{\theta} \\ & \quad + I_{zz_{\mathrm{ch}}}\cos^2\gamma\ddot{\theta} + \left(m_{\mathrm{ch}} h^2 + I_{xx_{\mathrm{ch}}} - I_{zz_{\mathrm{ch}}}\right)\sin 2\gamma \\ & \quad \times \dot{\theta}\dot{\gamma} + m_{\mathrm{ch}} h\,\left[-\sin\theta\,\sin\gamma\,\ddot{x} + \sin\gamma\cos\theta\,\ddot{y}\right] \\ & = l\,(\lambda_2 - \lambda_3) \end{aligned} \tag{13c}$$

$$I_{1_{\mathrm{w}}}\ddot{\varphi}_1 = \tau_1 + r_{\mathrm{w}}\lambda_2 \tag{13d}$$

$$I_{1_{\mathrm{w}}}\ddot{\varphi}_1 = \tau_2 + r_{\mathrm{w}}\lambda_3 \tag{13e}$$

$$\begin{aligned} & \left(m_{\mathrm{ch}} h^2 + I_{yy_{\mathrm{ch}}}\right)\ddot{\gamma} + m_{\mathrm{ch}} h\,(\ddot{x}\cos\theta + \ddot{y}\sin\theta \\ & \quad + \dot{y}\dot{\theta}\cos\theta)\cos\gamma \\ & \quad - \frac{1}{2}\left[-I_{xx_{\mathrm{ch}}} - m_{\mathrm{ch}} h^2 + I_{zz_{\mathrm{ch}}}\right]\dot{\theta}^2\sin 2\gamma \\ & \quad - m_{\mathrm{ch}} h\left[\dot{y}\dot{\theta}\,\cos\gamma\,\cos\theta\right] - m_{\mathrm{ch}} g h\sin\gamma \\ & = -\tau_1 - \tau_2 \end{aligned} \tag{13f}$$

where the parameter λ is the constraint force vector and τ_1 and τ_2 are torques acting on the left and the right wheels provided by the motors, respectively. Using the above equations, a new formulation for two-wheeled self-balancing robots is derived as equations (14), where u is the longitudinal linear velocity of the chassis ($\dot{x} = u\,\cos\theta$, $\dot{y} = u\,\sin\theta$).

$$\begin{aligned} & (3m_{\mathrm{w}} + m_{\mathrm{ch}})\,\dot{u} + h\,m_{\mathrm{ch}}(\ddot{\gamma}\cos\gamma - \dot{\gamma}^2\sin\gamma - \dot{\theta}^2\sin\gamma) \\ & = \frac{1}{r_{\mathrm{w}}}(\tau_1 + \tau_2) \end{aligned} \tag{14a}$$

$$\begin{aligned} & \Big[2\left(m_{\mathrm{w}} l^2 + I_{2_{\mathrm{w}}}\right) + I_{xx_{\mathrm{ch}}}\sin^2\gamma + m_{\mathrm{ch}}\, h^2\sin^2\gamma \\ & \quad + I_{zz_{\mathrm{ch}}}\cos^2\gamma + m_{\mathrm{w}} l^2\Big]\ddot{\theta} + \left(m_{\mathrm{ch}} h^2 + I_{xx_{\mathrm{ch}}} - I_{zz_{\mathrm{ch}}}\right) \\ & \quad \times \sin 2\gamma\,\dot{\theta}\dot{\gamma} + m_{\mathrm{ch}}\, h\,\sin\gamma\,\dot{\theta}\,u = -\frac{l}{r_{\mathrm{w}}}\tau_1 + \frac{l}{r_{\mathrm{w}}}\tau_2 \end{aligned} \tag{14b}$$

$$\begin{aligned} & \left(I_{yy_{\mathrm{ch}}} + m_{\mathrm{ch}} h^2\right)\ddot{\gamma} + m_{\mathrm{ch}} h\,\cos\gamma\,\dot{u} \\ & \quad - \frac{1}{2}\left[I_{xx_{\mathrm{ch}}} + m_{\mathrm{ch}} h^2 - I_{zz_{\mathrm{ch}}}\right]\sin 2\gamma\,\dot{\theta}^2 - m_{\mathrm{ch}} g h\sin\gamma \\ & \quad = -\tau_1 - \tau_2 \end{aligned} \tag{14c}$$

The main difference between this model and the commonly used models is the term '$m_{\mathrm{ch}} h\dot{\theta}\,u\,\sin\gamma$.' We will show that the effect of this term is significant on the response of the system.

2.3 Kane's approach

In this section, we show that the same results can be obtained using Kane's approach. In Kane's method [18, 19], the equations of motion can be derived as follows:

Generalized coordinates q_r are selected to define the position of all points and the orientation of all bodies of the multibody system.

$$q_r \ (r = 1, \ldots, N_0) \tag{15}$$

where N_0 is degrees of freedom.

Generalized speeds u_r are functions of $\dot{q}_i$ (time derivative of q_i). It is used to simplify the expressions for linear and angular velocities:

$$u_r = Z_r(q,t) + \sum_{i=1}^{N_0} Y_{ri}(q,t)\dot{q}_i \quad (1 < r < N_0) \tag{16}$$

where Y_{ri} and Z_r are functions of $q_1, \ldots, q_{N0}$ and the time t, whereas $u_r = \dot{q}_r$ is the straightforward and conspicuous definition. In our system, the generalized speeds are defined as follows:

$$u_1 = u, \quad u_2 = \dot{\theta}, \quad u_3 = \dot{\gamma} \tag{17}$$

Kane's method requires the computation of absolute velocities and accelerations. All calculations of the velocities and accelerations of the chassis are performed in the frame $X_{3_{ch}}Y_{3_{ch}}Z_{3_{ch}}$, and those of the wheels are performed in the frame $X_1Y_1Z_1$. The linear and angular velocities and accelerations of bodies are as (19–21), where B_1 and P_1 denote the body and the center of mass of the chassis, respectively. $B_i, i = 2, 3$, represents the body of the first and the second wheels, and P_i, $i = 2, 3$, is the center of mass of the first and second wheels, respectively.

$$\begin{aligned}\vec{v}^{P_1} &= (u_3 h + \cos\gamma\, u_1)\,\vec{\imath}_{3_{ch}} + u_2 h \sin\gamma\, \vec{\jmath}_{3_{ch}} \\ &\quad + u_1 \sin\gamma\, \vec{k}_{3_{ch}} \end{aligned} \tag{18a}$$

$$\vec{v}^{P_2} = (u_1 + l\,u_2)\vec{\imath}_1 \tag{18b}$$

$$\vec{v}^{P_3} = (u_1 - l\,u_2)\vec{\imath}_1 \tag{18c}$$

$$\vec{\omega}^{B_1} = -u_2 \sin\gamma\, \vec{\imath}_{3_{ch}} + u_3\, \vec{\jmath}_{3_{ch}} + u_2 \cos\gamma\, \vec{k}_{3_{ch}} \tag{19a}$$

$$\vec{\omega}^{B_2} = \left(\frac{u_1}{r_w} + \frac{l}{r_w}u_2\right)\vec{\jmath}_1 + u_2\vec{k}_1 \tag{19b}$$

$$\vec{\omega}^{B_3} = \left(\frac{u_1}{r_w} - \frac{l}{r_w}u_2\right)\vec{\jmath}_1 + u_2\vec{k}_1 \tag{19c}$$

$$\begin{aligned}\vec{a}^{P_1} &= \left(\cos\gamma\,\dot{u}_1 + h\,\dot{u}_3 - h\,\sin\gamma\,\cos\gamma\,u_2^2\right)\vec{\imath}_{3_{ch}} \\ &\quad + (h\,\sin\gamma\,\dot{u}_2 + hcos\,\gamma\,u_2u_3 + u_1\,u_2 \\ &\quad + h\,\cos\gamma u_2u_3)\vec{\jmath}_{3_{ch}} + \left(\sin\gamma\dot{u}_1 - hu_3^2\right. \\ &\quad \left. - h\,\sin^2\gamma u_2^2\right)\vec{k}_{3_{ch}} \end{aligned} \tag{20a}$$

$$\vec{a}^{P_2} = (\dot{u}_1 + l\,\dot{u}_2)\,\vec{\imath}_1 + (u_1 + l\,u_2)\,u_2\vec{\jmath}_1 \tag{20b}$$

$$\vec{a}^{P_3} = (\dot{u}_1 - l\,\dot{u}_2)\,\vec{\imath}_1 + (u_1 - l\,u_2)u_2\vec{\jmath}_1 \tag{20c}$$

$$\begin{aligned}\vec{\alpha}^{B_1} &= (-\dot{u}_2\,\sin\,\gamma - u_2u_3\,\cos\,\gamma)\,\vec{\imath}_{3_{ch}} + \dot{u}_3\vec{\jmath}_{3_{ch}} \\ &\quad + (\dot{u}_2\cos\,\gamma - u_2\,u_3\sin\,\gamma)\vec{k}_{3_{ch}} \end{aligned} \tag{21a}$$

$$\begin{aligned}\vec{\alpha}^{B_2} &= \left(\frac{\dot{u}_1}{r_w} + \frac{l}{r_w}\dot{u}_2\right)\vec{\jmath}_1 - \left(\frac{u_1}{r_w} + \frac{l}{r_w}u_2\right)u_2\vec{\imath}_1 \\ &\quad + \dot{u}_2\vec{k}_1 \end{aligned} \tag{21b}$$

$$\begin{aligned}\vec{\alpha}^{B_3} &= \left(\frac{\dot{u}_1}{r_w} - \frac{l}{r_w}\dot{u}_2\right)\vec{\jmath}_1 - \left(\frac{u_1}{r_w} - \frac{l}{r_w}u_2\right)u_2\vec{\imath}_1 \\ &\quad + \dot{u}_2\vec{k}_1 \end{aligned} \tag{21c}$$

where the vectors $\vec{\imath}$, $\vec{\jmath}$, and $\vec{k}$ with '3_{ch}' and '1' subscripts, denote unit vectors in the frames $X_{3_{ch}}Y_{3_{ch}}Z_{3_{ch}}$ and $X_1Y_2Z_3$, respectively.

Partial linear velocity $\vec{V}_r^{\,P}$ *and partial angular velocity* $\vec{\Omega}_r^{P}$ are time-varying linear functions of the $u_r's$ and can be expressed as:

$$\vec{V}_r^{\,P_i} = \frac{\partial \vec{v}^{P_i}}{\partial u_r} \tag{22}$$

$$\vec{\Omega}_r^{B_i} = \frac{\partial \vec{\omega}^{B_i}}{\partial u_r} \tag{23}$$

Utilizing (22–23), the partial linear and angular velocities are obtained as shown in Tables 2 and 3.

Table 2 Partial linear velocities

$\vec{V}_r^{\,P_i}$	$r = 1$	$r = 2$	$r = 3$
$i = 1$	$\cos\gamma\,\vec{\imath}_{3_{ch}} + \sin\gamma\,\vec{k}_{3_{ch}}$	$h\,\sin\gamma\,\vec{\jmath}_{3_{ch}}$	$h\,\vec{\imath}_{3_{ch}}$
$i = 2$	$\vec{\imath}_1$	$l\,\vec{\imath}_1$	0
$i = 3$	$\vec{\imath}_1$	$-l\,\vec{\imath}_1$	0

Table 3 Partial angular velocities

$\vec{\Omega}_r^{B_i}$	$r = 1$	$r = 2$	$r = 3$
$i = 1$	0	$-\sin\gamma\,\vec{\imath}_{3_{ch}} + \cos\gamma\,\vec{k}_{3_{ch}}$	$\vec{\jmath}_{3_{ch}}$
$i = 2$	$\frac{1}{r}\vec{\jmath}_1$	$+\frac{l}{r}\vec{\jmath}_1 + \vec{k}_1$	0
$i = 3$	$\frac{1}{r}\vec{\jmath}_1$	$-\frac{l}{r}\vec{\jmath}_1 + \vec{k}_1$	0

Table 4 Active forces and torques

	$i=1$	$i=2$	$i=3$
R_{P_i}	$-m_{\mathrm{ch}} g \cos\gamma\, \vec{k}_{3_{\mathrm{ch}}} + m_{\mathrm{ch}} g \sin\gamma\, \vec{\imath}_{3_{\mathrm{ch}}}$	$-m_{\mathrm{w}} g \vec{k}_1$	$-m_{\mathrm{w}} g \vec{k}_1$
M_{B_i}	$-(\tau_1+\tau_2)\vec{\jmath}_{3_{\mathrm{ch}}}$	$\tau_1 \vec{\jmath}_1$	$\tau_2 \vec{\jmath}_1$

Generalized active forces F_r are the active forces or torques inserting energy to the system. These forces might be external or internal.

$$F_r = \sum_{i=1}^{\kappa} \vec{V}_r^{P_i} \cdot \vec{R}_{P_i} + \sum_{j=1}^{\beta} \vec{\Omega}_r^{B_j} \cdot \vec{M}_{B_j} \quad (r = 1, \ldots, N_0) \tag{24}$$

$\vec{R}_{P_i}$ $(1 \le i \le \kappa)$ is the effect of κ contact and distance active forces and $\vec{M}_{B_j}$ $(1 \le j \le \beta)$ is the effect of β active torques. Active forces and torques for our system are presented in Table 4.

Generalized inertia forces F_r^* would rely on an equation of the form:

$$F_r^* = \sum_{i=1}^{\mu} V_r^{Pi} \cdot R_{p_i}^* + \sum_{j=1}^{\eta} \Omega_r^{B_j} \cdot T_{B_j}^* \quad (r = 1, \ldots, N_0) \tag{25}$$

where μ, η, $R_{p_i}^*$, and $T_{B_j}^*$ denote, respectively, the number of points retaining mass, the number of rigid bodies retaining inertia, inertia forces, and inertia torques. We have:

$$R_{p_i}^* \triangleq -m_{P_i} a^{P_i} \tag{26}$$

$$T_{B_j}^* \triangleq -\alpha^{B_j} . I^{\frac{Bj}{B_j^*}} - \omega^{B_j} \times I^{\frac{Bj}{B_j^*}} . \omega^{B_j} \tag{27}$$

where m_{P_i}, a^{P_i}, α^{B_j}, $I^{\frac{Bj}{B_j^*}}$, and ω^{B_j} denote the mass of P_i, acceleration of P_i, angular velocity of B_j, inertia dyadic of B_j about its mass center B_j^*, and the angular velocity of B_j, respectively. Kane's equation has the following form:

$$F_r^* + F_r = 0 \tag{28}$$

The dynamical formulations for two-wheeled self-balancing robots are derived as follows:

$$(3m_{\mathrm{w}} + m_{\mathrm{ch}})\,\dot{u} + h\, m_{\mathrm{ch}} \left(\ddot{\gamma}\cos\gamma - \dot{\gamma}^2 \sin\gamma - \dot{\theta}^2 \sin\gamma\right) = \frac{1}{r_{\mathrm{w}}}\,(\tau_1 + \tau_2) \tag{29a}$$

$$\left[2\left(m_{\mathrm{w}} l^2 + I_{2_{\mathrm{w}}}\right) + I_{xx_{\mathrm{ch}}} \sin^2\gamma + m_{\mathrm{ch}}\, h^2 \sin^2\gamma + I_{zz_{\mathrm{ch}}} \cos^2\gamma + m_{\mathrm{w}}\, l^2\right]\ddot{\theta} + \left(m_{\mathrm{ch}} h^2 + I_{xx_{\mathrm{ch}}} - I_{zz_{\mathrm{ch}}}\right)\, \sin 2\gamma\quad \dot{\theta}\dot{\gamma} + m_{\mathrm{ch}} h\, \sin\gamma\, \dot{\theta}\, u = -\frac{l}{r_{\mathrm{w}}}\tau_1 + \frac{l}{r_{\mathrm{w}}}\tau_2 \tag{29b}$$

$$\left(I_{yy_{\mathrm{ch}}} + m_{\mathrm{ch}} h^2\right)\ddot{\gamma} + m_{\mathrm{ch}} h\, \cos\gamma\, \dot{u} - \frac{1}{2}\left[I_{xx_{\mathrm{ch}}} + m_{\mathrm{ch}} h^2 - I_{zz_{\mathrm{ch}}}\right]\, sin2\gamma\, \dot{\theta}^2 - m_{\mathrm{ch}} g h \sin\gamma = -\tau_1 - \tau_2 \tag{29c}$$

These equations are identical to (14). As it mentioned before, there is a term which is neglected in Kim's model [15] and other commonly used two-wheeled robot's models. We will show the effects of the new term by some simulation results in the next section.

2.4 Open-loop simulation

In this section, the dynamical behavior of the robot is put on display. The main objective is to represent the effect of the term $'m_{\mathrm{ch}} h\dot{\theta}\, u\, \sin\gamma'$ on the behavior of the system, and to compare it with the case where this term is not considered. Let us define the former model as the '*conventional model*' (*CM*) and the model presented in this paper as the '*modified model*' (*MM*), and the term $'m_{\mathrm{ch}} h\dot{\theta}\, u\, \sin\gamma'$ as the modified term. Simulations are based on free response of the system with arbitrary initial conditions and no forcing. The robot parameters are shown in Table 5. The values are obtained from an experimental model of two-wheeled self-balancing robot, which we constructed in *Khaje Nasir University of Technology*.

The robot is considered to start moving from the origin of the horizontal plane. The pendulum is deviated from its downward position with the initial angle and angular velocity of γ_0 and $\dot{\gamma}_0$, respectively; furthermore, an initial longitudinal (forward) velocity of u_0 is applied to the chassis. If $\dot{\theta}$, the angular velocity of the chassis in the $x-y$ plane, were equal to zero, the simple situation of moving chassis of the robot on the straight line would happen; and by this assumption,

Table 5 Robot parameters

Property	Unit	Value	Definition
m_{ch}	kg	3.99	Mass of the chassis
m_w	kg	1.064	Mass of the wheel
Iyy_{ch}	kg m^2	0.043	Inertia moment of the chassis relative to axes $Y_{3_{ch}}$
Ixx_{ch}	kg m^2	0.068	Inertia moment of the chassis relative to axes $X_{3_{ch}}$
Izz_{ch}	kg m^2	0.044	Inertia moment of the chassis relative to axes $Z_{3_{ch}}$
I_{1w}	kg m^2	0.009	Inertia moment of the wheel relative to axes X_{4_w}
I_{2w}	kg m^2	0.043	Inertia moment of the wheel relative to axes Y_{4_w}
g	m^2 s^{-1}	9.81	Acceleration of gravity
r_w	m	0.3	Radius of the wheels
l	m	0.2	Half-distance between wheels
h	m	0.2	Distance from central point of the line between the two wheels to *CoG* of the chassis

Table 6 Initial conditions

Parameter	x_0	y_0	θ_0	γ_0	u_0	$\dot{\theta}_0$	$\dot{\gamma}_0$
Value	0	0	0	$\frac{\pi}{2}$	4	$\frac{\pi}{5}$	$\frac{\pi}{10}$
Unit	m	m	rad	rad	m s^{-1}	rad s^{-1}	$\frac{\text{rad}}{\text{s}}$

two-wheeled robot converts to cart and inverted pendulum. In that case, there is no difference between '*conventional model*' and '*modified model.*' For our case, the rotation of the chassis in $x-y$ plane is brought up assuming that $\dot{\theta}_0 \neq 0$ and equal to $\frac{\pi}{5}\left(\frac{\text{rad}}{s}\right)$. Therefore, it is conspicuous that $m_{ch} h\dot{\theta}\, u \sin\gamma \neq 0$ and dissimilarities between time domain response and phase portrait of '*modified model*' and '*conventional model*' are expected. Initial conditions are shown in Table 6. Figure 4 represents the path of the chassis, in $x-y$ plane, for '*modified*' and '*conventional models*' and Fig. 5 represents time response and phase domain portrait of parameters.

From Figs. 4 and 5, it is accessible that there are significant distinctions between '*modified*' and '*conventional*' models. The main difference is evident in Fig. 4 which depicted paths of '*modified*' and '*conventional*' models on the horizontal plane. It is noticeable that the system with '*conventional model*' moves on a circle, and however, the '*modified model*' moves on

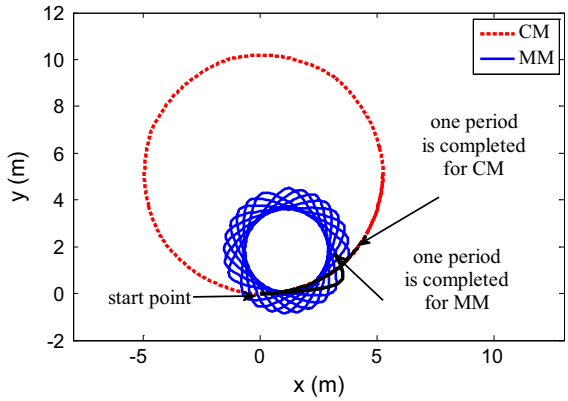

Fig. 4 Path for '*modified model*' (MM) and '*conventional model*' (CM) in horizontal plane

a quit different path. Its path is similar to *congruent rotated equilateral triangles* path.

Figure 5a, b exemplifies the time response of x and trajectory in the phase space for $\dot{x}-x$. In Fig. 5c, d the time response of y and phase portraits for $y-\dot{y}$ are represented. Figure 5e, f illustrates time response of θ and phase portrait for $\theta-\dot{\theta}$. It is seen that there is transparent difference between the responses of the *'conventional'* and *'modified models'*. Figure 5g, k exemplifies time response of γ and its trajectory in phase space.

The total energy function is acquired by summation of the kinetic energy (11) and the potential energy (12). We assume that the potential energy of the system is equal to zero when the pendulum is vertically downward. Figure 6 shows the total energy of both systems. The initial kinetic and potential energies of the system are equal to 57.57 and 9.78, respectively. Accordingly, total energy of the system is equal to 67.35. From Fig. 6, it is obvious that total energy level of '*modified model*' is constant during simulation time and equal to the initial energy value, but the total energy of the '*conventional model*' is varying with time. It means that consistency of energy level exists for '*modified model*,' but not for the '*conventional model.*' It is a second proof that the dynamical equations and simulations which are obtained in this paper are correct and the term '$m_{ch}\, h\dot{\theta}\, u \sin\gamma'$ has an important role in dynamical behavior of the two-wheeled robots.

3 Control system design

In this section, sliding-mode control techniques are used to derive the controllers. The controller objec-

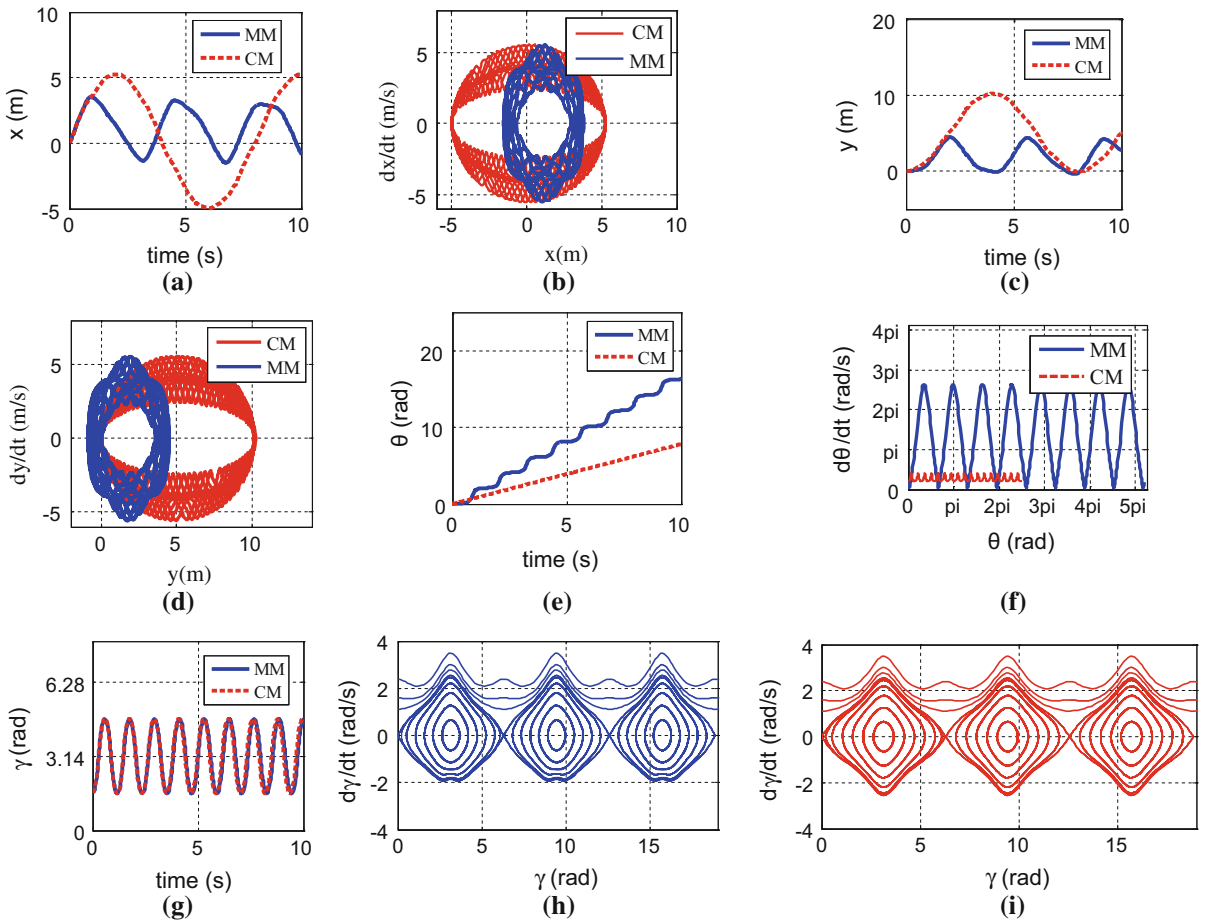

Fig. 5 **a** Position (x direction) versus time for '*modified model*' (MM) and '*conventional model*' (CM). **b** Phase portrait for x, $\dot{x}$ for '*modified model*' (MM) and '*conventional model*' (CM) (simulation time 100 s). **c** Position (y direction) versus time for '*modified model*' (MM) and '*conventional model*' (CM). **d** Phase portrait for y, $\dot{y}$ for '*modified model*' (MM) and '*conventional model*' (CM) (simulation time 100 s). **e** Steering angle of the chassis (θ) versus time for '*modified model*' (MM) and '*conventional model*' (CM). **f** Phase portrait for $\theta, \dot{\theta}$, for '*modified model*' (MM) and '*conventional model*' (CM) (simulation time 100 s). **g** Inclination angle of the chassis (γ) versus time for '*modified model*' and '*conventional model*.' **h** Phase portrait for γ, $\dot{\gamma}$ for '*modified model*' (MM). **k** Phase portrait for γ, $\dot{\gamma}$ for '*conventional model*' (CM)

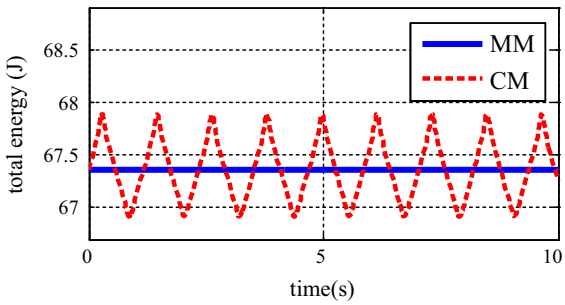

Fig. 6 Total energy versus time for '*modified model*' (MM) and '*conventional model*' (CM)

tive is to derive the two-wheeled self-balancing robot to the desired path as well as to make the robot stable. We are going to show that if we ignore the nonlinear coupling term in designing the controller, the controller cannot compensate the nonlinear coupling term's effect. For control design dynamical equations of two-wheeled self-balancing robots, i.e., Eq. (29) is rewritten in the following form:

$$\dot{u} = \Lambda_u \dot{\theta}^2 + \Psi_u \dot{\gamma}^2 + X_u(\tau_1 + \tau_2) + \Phi_u g \tag{30a}$$

$$\dot{\gamma} = \Lambda_\gamma \dot{\theta}^2 + \Psi_\gamma \dot{\gamma}^2 + X_\gamma(\tau_1 + \tau_2) + \Phi_\gamma g \tag{30b}$$

$$\ddot{\theta} = \Lambda_\theta\, \dot{\theta} u + \Psi_\theta\, \dot{\gamma}\dot{\theta} + X_\theta(\tau_1 - \tau_2) \tag{30c}$$

where Λ_u, Ψ_u, X_u, Φ_u, Λ_γ, Ψ_γ, X_γ, Φ_γ, Λ_θ, Ψ_θ and X_θ are defined in Appendix 2.

For the control system design, the idea of sliding-mode controller based on zero-dynamics theory is used [8]. By defining $\tau_1 - \tau_2 = \tau_\mathrm{w}$ and $\tau_1 + \tau_2 = \tau_v$, the system converts to two subsystems: the longitudinal subsystem and the rotational subsystem. The longitudinal subsystem consists of the first two equations of the vehicle dynamics, called the $\{u, \gamma\}$-subsystem, and the rotational subsystem consists of the third equation of the vehicle dynamics called the $\{\theta\}$-subsystem. $\{u, \gamma\}$-subsystem with τ_v as the control input and two degrees of freedom is an under actuated subsystem, while $\{\theta\}$-subsystem with τ_w as the control input and one degree of freedom is an actuated subsystem. The $\{u, \gamma\}$-subsystem can be written as:

$$\begin{cases} \dot{u} = \Lambda_u \dot{\theta}^2 + \Psi_u \dot{\gamma}^2 + X_u \tau_v + \Phi_u g \\ \ddot{\gamma} = \Lambda_\gamma \dot{\theta}^2 + \Psi_\gamma \dot{\gamma}^2 + X_\gamma \tau_v + \Phi_{\gamma g} \end{cases} \tag{31}$$

And the $\{\theta\}$-subsystem can be written as:

$$\ddot{\theta} = \Lambda_\theta\, \dot{\theta} u + \Psi_\theta\, \dot{\gamma}\dot{\theta} + X_\theta \tau_\mathrm{w} \tag{32}$$

The sliding-mode control techniques are used to derive the controllers since they are insensitive to parameter variation and uncertain disturbance. The inclination angle γ is controlled by the torque τ_v, and the rotational angle θ is controlled by the torque τ_w. While the longitudinal velocity u cannot be controlled directly, the inclination angle of the pendulum has a direct influence on it. As a result based on the nonlinear dynamic theory, we have used zero dynamics, where the inclination angle of the robot is considered as zero dynamics where the longitudinal acceleration, i.e., $\dot{u}_d$, is taken as the control input [8]. With the appropriate controller, the zero-dynamics subsystem would be stable. As a result, the overall controller is considered as three subcontrollers: rotational controller, longitudinal controller, and zero-dynamics controller. The error states for control design are defined as follows:

$$\begin{aligned} &e_1 = \theta - \theta_d, \quad e_2 = \dot{\theta} - \dot{\theta}_d, \quad e_3 = \xi - \xi_d, \\ &e_4 = u - u_d, \quad e_5 = \gamma - \gamma_d, \quad e_6 = \dot{\gamma} - \dot{\gamma}_d \end{aligned} \tag{33}$$

To achieve the control objective, the error differential equation of the $\{u, \gamma\}$-subsystem can be expressed as follows:

$$\begin{cases} \dot{e}_3 = e_4 \\ \dot{e}_4 = \Lambda_u \dot{\theta}^2 + \Psi_u \dot{\gamma}^2 + X_u \tau_v + \Phi_u g - \dot{u}_d \\ \dot{e}_5 = e_6 \\ \dot{e}_6 = \Lambda_\gamma\, \dot{\theta}^2 + \Psi_\gamma \dot{\gamma}^2 + X_\gamma \tau_v + \Phi_\gamma g - \ddot{\gamma}_d \end{cases} \tag{34}$$

Similarly, the error differential equation of the $\{\theta\}$-subsystem is as follows:

$$\begin{cases} \dot{e}_1 = e_2 \\ \dot{e}_2 = \Lambda_\theta\, \dot{\theta} u + \Psi_\theta\, \dot{\gamma}\dot{\theta} + X_\theta \tau_\mathrm{w} \end{cases} \tag{35}$$

3.1 Longitudinal control

In longitudinal control, the control objective is controlling the inclination angle of the body by the torque τ_v. Longitudinal motion is coupled with the inclination angle of the body. The longitudinal velocity cannot be directly controlled, but the inclination angle affects it directly. In order to apply the sliding-mode control technique, we can define sliding surface as

$$s_1 = \dot{e}_3 + c_1 e_3 \tag{36}$$

where c_1 is positive, then we can differentiate the sliding surface with respect to time as

$$\begin{aligned} \dot{s}_1 = \ddot{e}_3 + c_1 \dot{e}_3 = {} & \Lambda_u \dot{\theta}^2 + \Psi_u \dot{\gamma}^2 + X_u \tau_v \\ & + \Phi_u g - \dot{u}_d + c_1 \dot{e}_3 \end{aligned} \tag{37}$$

By adopting the exponential approach law, i.e., $\dot{s}_1 = -k_1 \mathrm{sgn}(s_1) - k_2 s_1$, the controller could be designed as follows:

$$\begin{aligned} \tau_v = {} & -\frac{\Lambda_u}{X_u}\, \dot{\theta}^2 - \frac{\Psi_u}{X_u}\, \dot{\gamma}^2 - \frac{\Phi_u}{X_u} g + \frac{\dot{u}_d}{X_u} \\ & - \frac{k_1}{X_u} \mathrm{sgn}\,(s_1) - \frac{k_2}{X_u}\, s_1 \end{aligned} \tag{38}$$

where k_1 and k_2 are positive design constants.

3.2 Zero-dynamics controller

The longitudinal position and inclination angle variables should be controlled by the only control input τ_v. To deal with this underactuated problem, we can get the zero-dynamics subsystem by setting the longitudinal position error $e_3 = \xi - \xi_d$ as zero, i.e., $e_3 = 0$ and then $\dot{e}_4 = 0$, where ξ is the displacement of the vehicle along the direction of the longitudinal velocity. From (31), we have τ_v as follows:

$$\tau_v = -\frac{\Lambda_u}{X_u}\, \dot{\theta}^2 - \frac{\Psi_u}{X_u}\, \dot{\gamma}^2 - \frac{\Phi_u}{X_u} g + \frac{\dot{u}_d}{X_u} \tag{39}$$

Substituting τ_v into the tracking error of $\dot{e}_6$ and the fact that $\ddot{\gamma} = \dot{e}_6 + \ddot{\gamma}_d$, the zero-dynamics subsystem is obtained as (40).

$$\ddot{\gamma} = \left(\Lambda_\gamma - \frac{X_\gamma \Lambda_u}{X_u}\right)\dot{\theta}^2 - \frac{C_u}{A_\gamma}g + \frac{X_\gamma \dot{u}_d}{X_u} \tag{40}$$

The control objective for designing zero-dynamics controller is finding an appropriate expression for the $\dot{u}_d$ as an input of longitudinal control, i.e., T_v. The sliding surface for zero-dynamics subsystem can be given by:

$$s_2 = \dot{e}_5 + c_2 e_5 \tag{41}$$

where c_2 is positive, then we can differentiate the sliding surface with respect to time as

$$\dot{s}_2 = \ddot{e}_5 + c_2\dot{e}_5 = \left(\Lambda_\gamma - \frac{X_\gamma \Lambda_u}{X_u}\right)\dot{\theta}^2 - \frac{C_u}{A_\gamma}g + \frac{X_\gamma \dot{u}_d}{X_u} - \ddot{\gamma}_d + c_2\dot{e}_5 \tag{42}$$

By adopting the exponential approach law, i.e., $\dot{s}_2 = -k_3\mathrm{sgn}(s_2) - k_4 s_2$, the controller could be designed as follows:

$$\dot{u}_d = \frac{X_u}{X_\gamma}\left[\left(\frac{X_\gamma \Lambda_u}{X_u} - \Lambda_\gamma\right)\dot{\theta}^2 + \frac{C_u}{A_\gamma}g + \ddot{\gamma}_d - c_2\dot{e}_5 - k_3\mathrm{sgn}\,(s_2) - k_4 s_2\right] \tag{43}$$

where k_3 and k_4 are positive design constants.

3.3 Rotational control

In this section, the control objective is to design a control strategy that permits the two-wheeled vehicle to track its desired path. The rotational angle θ is controlled by the torque τ_w directly in the $\{\theta\}$-subsystem. The sliding surface for rotational control is defined as follows:

$$s_3 = \dot{e}_1 + c_3 e_1 \tag{44}$$

$$\dot{s}_3 = \ddot{e}_1 + c_3\dot{e}_1 = \Lambda_\theta\,\dot{\theta}u + \Psi_\theta\,\dot{\gamma}\dot{\theta} + X_\theta\tau_\mathrm{w} - \ddot{\theta}_d + c_3\dot{e}_1, \tag{45}$$

By adopting the exponential approach law, i.e., $\dot{s}_3 = -k_5\mathrm{sgn}(s_2) - k_6 s_2$, the controller could be designed as follows:

$$\tau_\mathrm{w} = -\frac{\Lambda_\theta}{X_\theta}\,\dot{\theta}u - \frac{\Psi_\theta}{X_\theta}\dot{\gamma}\dot{\theta} + \frac{1}{X_\theta}\ddot{\theta}_d - \frac{c_3}{X_\theta}\,\dot{e}_1 - \frac{k_5}{X_\theta}\mathrm{sgn}(s_3) - \frac{k_6}{X_\theta}\,s_3 \tag{46}$$

3.4 Closed-loop simulation

To evaluate the effectiveness of the proposed controller laws, a simulation study is carried out in this section. In this simulation, the initial conditions are supposed as $x_0 = 0\,\mathrm{m}$, $y_0 = 0\,\mathrm{m}$, $\theta_0 = 0\,\mathrm{rad}$, $\dot{\theta}_0 = 0\,\mathrm{rad/s}$, $\gamma_0 = \frac{\pi}{4}\,\mathrm{rad}$, $\dot{\gamma}_0 = 0\,\mathrm{rad/s}$, $u_0 = 0\,\mathrm{m/s}$. The desired value of the inclination angle and inclination angular velocity is zero, i.e., $\gamma_d = 0\,\mathrm{rad}$, $\dot{\gamma}_d = 0\,\mathrm{rad/s}$, and the desired trajectory for rotational angular velocity is given as $\dot{\theta}_d = 1\,\mathrm{rad/s}$. To achieve the control objectives, the coefficients of the controllers are designed as $k_1 = 2$, $k_2 = 4$, $k_3 = k_5 = 0.4$, $k_4 = k_6 = 0.2$, $c_1 = c_2 = c_3 = 0.4$.

For the study of the effect of the $'m_{\mathrm{ch}}h\dot{\theta}\,u\,\sin\gamma'$ term, two simulations have been conducted. In the first simulation, the proposed controller is applied to the '*modified model*' (see Figs. 7a, 8a, 9a, 10a), and in the second simulation, a controller based on conventional equation is applied to the '*modified model*' (see Figs. 7b, 8b, 9b, 10b). This controller is the same as the first controller except in τ_w which does not contain the

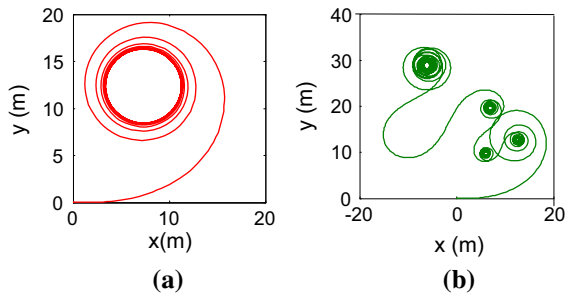

Fig. 7 Trajectory tracking of the robot on x–y plane. **a** '*modified model*' with the controller based on '*modified model.*' **b** '*modified model*' with the controller based on '*conventional model*'

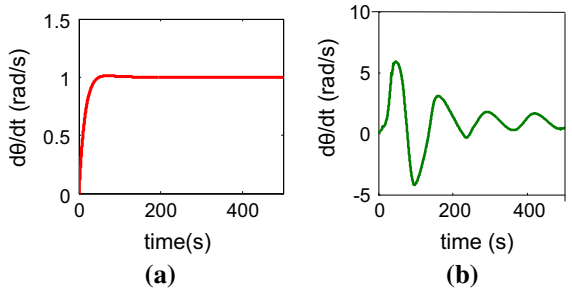

Fig. 8 Steering angular velocity of the chassis ($\dot{\theta}$) versus time. **a** '*modified model*' with the controller based on '*modified model.*' **b** '*modified model*' with the controller based on '*conventional model*'

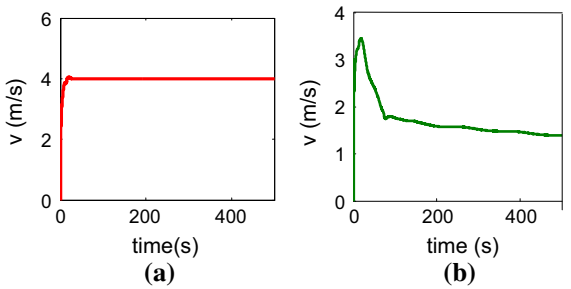

Fig. 9 Longitudinal velocity of the chassis (u) versus time. **a** '*modified model*' with the controller based on '*modified model*.' **b** '*modified model*' with the controller based on '*conventional model*'

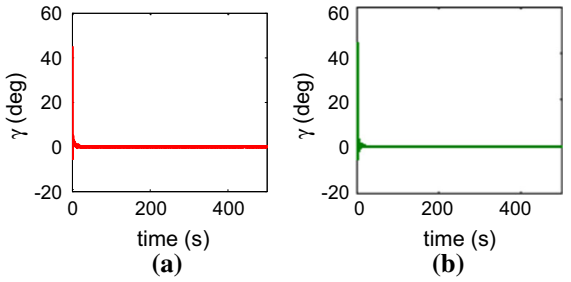

Fig. 10 Inclination angle of the chassis (γ) versus time. **a** '*modified model*' with the controller based on '*modified model*.' **b** '*modified model*' with the controller based on '*conventional model*'

term: $'-\frac{\Lambda_\theta}{X_\theta}\dot{\theta}u'$. Path tracking of the two-wheeled robot on the $x--y$ plane is plotted in Fig. 7. Figure 8 shows the steering angular velocity. The longitudinal velocity of the chassis is plotted in Fig. 9, and the inclination angle is plotted in Fig. 10. The result demonstrates that if we apply a controller based on the '*modified model,*' the inclination angle of the robot is stable (see Fig. 10a); the robot ultimately tracks an approximate circle (see Figs. 7a, 8a). But if we ignore the *modified term* in the controller design, the inclination angle of the robot is stable (see Fig. 10b), and however, the system could not follow the desired path (see Figs. 7a, 8a). As it is shown, the existence of the *modified term* affects the path tracking control of the system significantly. As a result, this nonlinear coupling term is important, and if we ignore it, in designing the controller, the controller cannot compensate its effect.

4 Conclusion

This paper is devoted to the dynamical analysis of two-wheeled self-balancing robots. We obtained a modified dynamical formulation of the system by two methods, Kane's approach and Lagrangian method. Both approaches result in the same formulation. Our model is more detailed compared with the '*conventional models*.' The most important difference is the appearance of a new term, $'m_{\mathrm{ch}}h\dot{\theta}\,u\,\sin\gamma'$, in the dynamical equations. The importance of this term and its effects on the behavior of the system are shown by different simulations. Meaningful distinction is observed between the *modified* and the '*conventional models*.' It is also shown that the total energy of the system remains constant only for the '*modified model*,' which is a second proof that our dynamical equations and simulations are correct. Then by applying sliding-mode controllers, it is shown that the existence of the new term, $'m_{\mathrm{ch}}h\dot{\theta}\,u\,\sin\gamma'$ affects the path tracking control of the system significantly. As a result, this nonlinearity is important, and if we ignore it, in designing the controller, the controller cannot compensate its effect.

Appendix 1

Transform matrixes and relative linear and angular velocities related to the chassis and the wheels are presented as

$$ {}^{0}_{1}T = \begin{bmatrix} \cos\theta & -\sin\theta & 0 & x \\ \sin\theta & \cos\theta & 0 & y \\ 0 & 0 & 1 & r_{\mathrm{w}} \\ 0 & 0 & 0 & 1 \end{bmatrix} \tag{47} $$

$$ {}^{1}_{2\mathrm{ch}}T = \begin{bmatrix} \cos\gamma & 0 & \sin\gamma & 0 \\ 0 & 1 & 0 & 0 \\ -\sin\gamma & 0 & \cos\gamma & 0 \\ 0 & 0 & 0 & 1 \end{bmatrix} \tag{48} $$

$$ {}^{2\mathrm{ch}}_{3\mathrm{ch}}T = \begin{bmatrix} 1 & 0 & 0 & 0 \\ 0 & 1 & 0 & 0 \\ 0 & 0 & 1 & h \\ 0 & 0 & 0 & 1 \end{bmatrix} \tag{49} $$

$$ {}^{0}_{1}v = \begin{bmatrix} \dot{x} \\ \dot{y} \\ 0 \end{bmatrix}, \quad {}^{1}_{2\mathrm{ch}}v = \begin{bmatrix} 0 \\ 0 \\ 0 \end{bmatrix}, {}^{2\mathrm{ch}}_{3\mathrm{ch}}v = \begin{bmatrix} 0 \\ 0 \\ 0 \end{bmatrix} \tag{50} $$

$$ {}^{0}_{1}\Omega = \begin{bmatrix} 0 \\ 0 \\ \dot{\theta} \end{bmatrix}, {}^{1}_{2\mathrm{ch}}\Omega = \begin{bmatrix} 0 \\ \dot{\gamma} \\ 0 \end{bmatrix}, {}^{2\mathrm{ch}}_{3\mathrm{ch}}\Omega = \begin{bmatrix} 0 \\ 0 \\ 0 \end{bmatrix} \tag{51} $$

$$
{}^{1}_{2_{\mathrm{w}}}T = \begin{bmatrix} \cos\alpha & -\sin\alpha & 0 & l\cos\alpha \\ \sin\alpha & \cos\alpha & 0 & l\sin\alpha \\ 0 & 0 & 1 & 0 \\ 0 & 0 & 0 & 1 \end{bmatrix} \tag{52}
$$

$$
{}^{2_{\mathrm{w}}}_{3_{\mathrm{w}}}T = \begin{bmatrix} 1 & 0 & 0 & 0 \\ 0 & \cos\varphi & -\sin\varphi & 0 \\ 0 & \sin\varphi & \cos\varphi & 0 \\ 0 & 0 & 0 & 1 \end{bmatrix} \tag{53}
$$

$$
{}^{3_{\mathrm{w}}}_{4_{\mathrm{w}}}T = \begin{bmatrix} 1 & 0 & 0 & 0 \\ 0 & 1 & 0 & r_{\mathrm{w}} \\ 0 & 0 & 1 & 0 \\ 0 & 0 & 0 & 1 \end{bmatrix} \tag{54}
$$

$$
{}^{0}_{1}v = \begin{bmatrix} \dot{x} \\ \dot{y} \\ 0 \end{bmatrix}, {}^{1}_{2_{\mathrm{w}}}v = {}^{2_{\mathrm{w}}}_{3_{\mathrm{w}}}v = {}^{3_{\mathrm{w}}}_{4_{\mathrm{w}}}v = \begin{bmatrix} 0 \\ 0 \\ 0 \end{bmatrix} \tag{55}
$$

$$
{}^{0}_{1}\Omega = \begin{bmatrix} 0 \\ 0 \\ \dot{\theta} \end{bmatrix}, {}^{2_{\mathrm{w}}}_{3_{\mathrm{w}}}\Omega = \begin{bmatrix} \dot{\varphi} \\ 0 \\ 0 \end{bmatrix}, {}^{1}_{2_{\mathrm{w}}}\Omega = {}^{3_{\mathrm{w}}}_{4_{\mathrm{w}}}\Omega = \begin{bmatrix} 0 \\ 0 \\ 0 \end{bmatrix} \tag{56}
$$

where 0, 1, 2_{ch}, 3_{ch}, 2_{w}, 3_{w}, and 4_{w} denote, respectively, the frames $X_0Y_0Z_0$, $X_1Y_1Z_1$, $X_{2_{\mathrm{ch}}}Y_{2_{\mathrm{ch}}}Z_{2_{\mathrm{ch}}}$, $X_{3_{\mathrm{ch}}}Y_{3_{\mathrm{ch}}}Z_{3_{\mathrm{ch}}}$, $X_{2_{\mathrm{w}}}Y_{2_{\mathrm{w}}}Z_{2_{\mathrm{w}}}$, $X_{3_{\mathrm{w}}}Y_{3_{\mathrm{w}}}Z_{3_{\mathrm{w}}}$ and $X_{4_{\mathrm{w}}}Y_{4_{\mathrm{w}}}Z_{4_{\mathrm{w}}}$.

Appendix 2

$$
\Lambda_u = \frac{-B_uC_\gamma - A_\gamma C_u}{A_uA_\gamma - B_uB_\gamma}, \quad \Psi_u = -\frac{C_uA_\gamma}{A_uA_\gamma - B_uB_\gamma},
$$

$$
X_u = \frac{A_\gamma/r_{\mathrm{w}} + B_u}{A_uA_\gamma - B_uB_\gamma}, \quad \Phi_u = \frac{B_uD_\gamma}{A_uA_\gamma - B_uB_\gamma},
$$

$$
\Lambda_\gamma = \frac{-C_\gamma A_u + B_uC_u}{A_uA_\gamma - B_uB_\gamma}, \quad \Psi_\gamma = \frac{B_\gamma C_u}{A_uA_\gamma - B_uB_\gamma},
$$

$$
X_\gamma = \frac{-\frac{B_\gamma}{r_{\mathrm{w}}} - A_u}{A_uA_\gamma - B_uB_\gamma}, \quad \Phi_\gamma = -\frac{A_uD_\gamma}{A_uA_\gamma - B_uB_\gamma},
$$

$$
\Lambda_\theta = \frac{B_\theta}{A_\theta}, \quad \Psi_\theta = \frac{C_\theta}{A_\theta}, \quad X_\theta = \frac{D_\theta}{A_\theta},
$$

$$
A_u = 3m_{\mathrm{w}} + m_{\mathrm{ch}}, \quad B_u = h\, m_{\mathrm{ch}}\cos\gamma,
$$

$$
C_u = -h\, m_{\mathrm{ch}}\sin\gamma, \quad A_\gamma = I_{yy_{\mathrm{ch}}} + m_{\mathrm{ch}}h^2,
$$

$$
B_\gamma = h\, m_{\mathrm{ch}}\cos\gamma,
$$

$$
C_\gamma = -\frac{1}{2}\left[I_{xx_{\mathrm{ch}}} + m_{\mathrm{ch}}h^2 - I_{zz_{\mathrm{ch}}}\right]\sin 2\gamma,
$$

$$
D_\gamma = -\mathrm{h}\ \mathrm{m}_{\mathrm{ch}}\sin\gamma,
$$

$$
A_\theta = \left[2\left(m_{\mathrm{w}}l^2 + I_{2_{\mathrm{w}}}\right) + I_{xx_{\mathrm{ch}}}\sin^2\gamma + m_{\mathrm{ch}}h^2\sin^2\gamma + I_{zz_{\mathrm{ch}}}\cos^2\gamma + m_{\mathrm{w}}l^2\right],
$$

$$
B_\theta = -m_{\mathrm{ch}}h\sin(\gamma),
$$

$$
C_\theta = -\left(m_{\mathrm{ch}}h^2 + I_{xx_{\mathrm{ch}}} - I_{zz_{\mathrm{ch}}}\right)\sin(2\gamma),
$$

$$
D_\theta = \frac{1}{r_{\mathrm{w}}},
$$

References

1. Grasser, F., Arrigo, A.D., Colombi, S., Silvio, A.C.: JOE: a mobile, inverted pendulum. IEEE Trans. Ind. Electron. **49**(1), 107–114 (2002)
2. Vermeiren, L., Dequidt, A., Guerra, T.M., Rago-Tirmant, H., Parent, M.: Modeling, control and experimental verification on a two-wheeled vehicle with free inclination: an urban transportation system. Control Eng. Pract. **19**(7), 744–756 (2011)
3. Segway Inc.: Reference manual, Segway personal transporter (PT). Segway Inc., Bedford, NH (2006)
4. Ravichandran, M.T., Mahindrakar, A.D.: Robust stabilization of a class of underactuated mechanical systems using time scaling and Lyapunov redesign. IEEE Trans. Ind. Electron. **58**(9), 4299–4313 (2011)
5. Maddahi, A., Shamekhi, A.H., Ghaffari, A.: A Lyapunov controller for self-balancing two-wheeled vehicles. Robotica **33**(01), 225–239 (2015)
6. Huang, J., Guan, Z.H., Matsuno, T., Fukuda, T., Sekiyama, K.: Sliding-mode velocity control of mobile-wheeled inverted-pendulum systems. IEEE Trans. Robot. **26**(4), 750–758 (2010)
7. Cui, R., Guo, J., Mao, Z.: Adaptive backstepping control of wheeled inverted pendulums models. Nonlinear Dyn. **79**(1), 501–511 (2015)
8. Yue, M., Wei, X., Li, Z.: Adaptive sliding-mode control for two-wheeled inverted pendulum vehicle based on zero-dynamics theory. Nonlinear Dyn. **76**(1), 459–471 (2014)
9. Yue, M., Wei, X., Li, Z.: Zero-dynamics-based adaptive sliding mode control for a wheeled inverted pendulum with parametric friction and uncertain dynamics compensation. Trans. Inst. Meas. Control. (2014). doi:10.1177/0142331214532999
10. Goher, K., Ahmad, S., Tokhi, O.M.: A new configuration of two wheeled vehicles: towards a more workspace and motion flexibility. In: *4th system conference. IEEE*. San Diego, CA (2010)
11. Larimi, S.R., Zarafshan, P., Moosavian, S.A.A.: A new stabilization algorithm for a two-wheeled mobile robot aided by reaction wheel. J. Dyn. Syst. Meas. Control **137**(1), 011009 (2015)
12. Almeshal, A.M., Goher, K.M., Tokhi, M.O.: Dynamic modelling and stabilization of a new configuration of two-wheeled machines. Robot. Auton. Syst. **61**(5), 443–472 (2013)

13. Huang, J., Ding, F., Fukuda, T., Matsuno, T.: Modeling and velocity control for a novel narrow vehicle based on mobile wheeled inverted pendulum. IEEE Trans. Control Syst. Technol. **21**(5), 1607–1617 (2013)
14. Pathak, K., Franch, J., Agrawal, S.K.: Velocity and position control of a wheeled inverted pendulum by partial feedback linearization. IEEE Trans. Robot. **21**(3), 505–513 (2005)
15. Kim, Y., Kim, S.H., Kwak, Y.K.: Dynamic analysis of a nonholonomic two-wheeled inverted pendulum robot. J. Intell. Robot. Syst. **44**(1), 25–46 (2005)
16. Siegwart, R., Nourbakhsh, I.R., Scaramuzza, D.: Introduction to Autonomous Mobile Robots. MIT press, Cambridge (2004)
17. Lanczos, C.: The Variational Principle of Mechanics, 3rd edn. University of Toronto Press, Toronto (1966)
18. Kane, T.R., Levinson, D.A.: Dynamics: Theory and Applications. McGraw-Hill, New York (1985)
19. Kane, T.R., Levinson, D.A.: The use of Kane's dynamical equations in robotics. Int. J. Robot. Res. **2**(3), 3–21 (1983)